Localization of GNSS RFI Transmitters Using Digital Surface Models

Maurizio Scaramuzza
Dr. sc. techn. ETHZ
skyguide, Swiss Air Navigation Services Ltd.
CH-8602 Wangen bei Dübendorf, Switzerland
Fax: +41 43 931 66 19
E-Mail: maurizio.scaramuzza@skyguide.ch

ABSTRACT

GNSS radio frequency interference (RFI) is increasingly becoming an important topic with the growth of applications based on these systems. Furthermore, safety critical applications exposed to RFI might lead to unacceptable performance degradations. In a first step it is therefore crucial to develop the capability of detecting potential GNSS RFI. In a second step it is necessary to develop the ability of localizing the GNSS RFI transmitter.

Related to the first step, a methodology for the detection of potential GNSS RFI was presented at the IFIS 2014 in Oklahoma City, OK [1], and at the ION GNSS+ 2015 in Tampa, FL [2]. This method is primarily based on GPS L1 Carrier to Noise Power Ratio (C/N_0) measurements recorded onboard of helicopters.

Concerning the second step the advantage is taken that the helicopters are flying at low altitudes above ground level. Consequently it is expected that these aerial vehicles are only partially affected by interference sources due to terrain shadowing effects. This circumstance can be utilized to draw conclusions on the potential location of the GNSS RFI transmitter. To do so, digital surface models, electromagnetic signal propagation models and GNSS signal degradation information is used in order to confine the location of the GNSS RFI transmitter.

After a short recapitulation on the methodology used to detect potential GNSS RFI, an approach for GNSS RFI transmitter localization is presented.

INTRODUCTION

The method for the detection of potential GPS RFI consists in installing mini quick access recorders (mQAR) on board of two dozen helicopters and collecting data during a period of several years. The helicopter fleets are operated by Rega, the main Swiss Helicopter Emergency and Medical Service (HEMS), and by the Swiss Air Force (SAF). Daily missions of those two operators are used for data recording, so there is a random coverage of large parts of Switzerland. Since those helicopter missions are all flying at low altitudes (90% of flight time below 500m AGL), it is expected that they have a higher probability of being exposed to ground based RFI than commercial fixed wing operations.

For RFI detection it would be advantageous to record parameters such as the receiver's Auto Gain Control (AGC) or the power spectrum density within the L1 band, but only data on the ARINC 429 bus is available and therefore the only recorded parameter relating to the GPS signal quality are the C/N_0. These are then normalized based on GPS satellite azimuth and elevation angles as well as roll, pitch and yaw angles of the helicopters. To do so it is necessary to know the expected $C/N_{0,exp}$ at each GPS signal incidence angle at the receiver antenna. This was empirically derived by assessing over 200 hours of recorded data of each helicopter, resulting in an antenna pattern as depicted in Figure 1. For more details refer to [2].

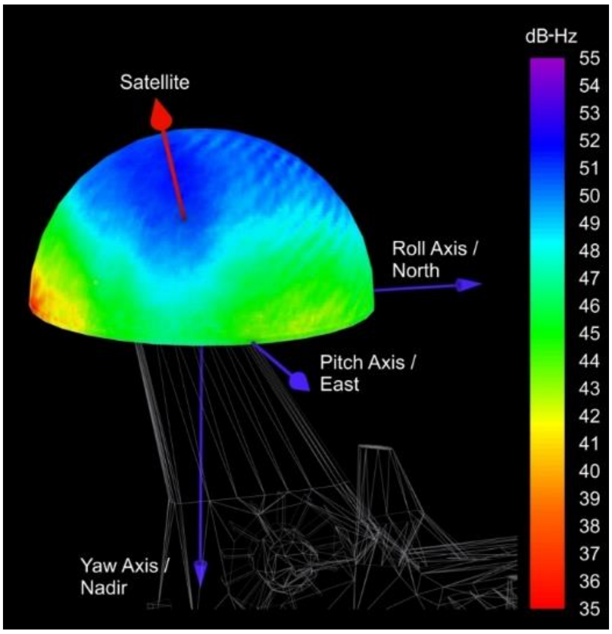

Figure 1: GPS antenna pattern on top of a helicopter fin describing the $C/N_{0,exp}$. The red arrow indicates the direction towards an arbitrary GPS satellite (incidence angle of GPS signal).

Finally, the normalized GPS signals are statistically assessed for the determination of potential RFI. Only GPS L1 C/A signals are taken into account, but with a few modifications this method can be adapted to any GNSS providing pseudo range services. This method has shown, based on assessments of over 6000 flight hours, that C/N_0 degradations due to potential GPS RFI of a few dB can be detected. One example is shown in Figure 2, where the C/N_0 ratios of all tracked satellites were similarly affected by a potentially interfering signal.

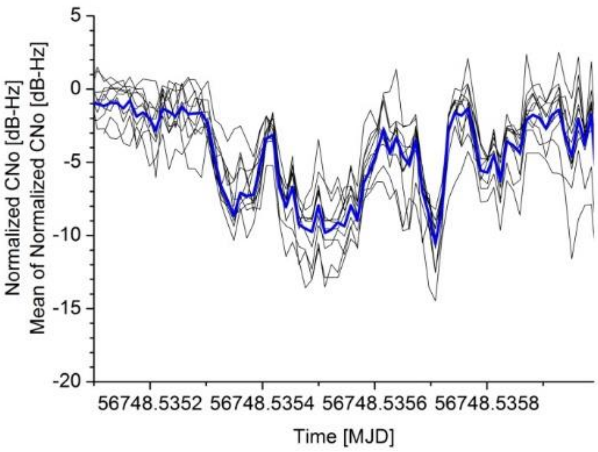

Figure 2: Situation where a potential RFI might be present. The thin black lines represents the normalized C/N_0 of each tracked satellite where the bold blue line is derived by averaging the normalized C/N_0.

Within the assessed period, degradations of normalized C/N_0 were observed at different locations. A repeatedly degraded C/N_0 at the same location is a strong indicator for a static RFI source in the vicinity of the flight paths. One of these areas is shown in Figure 3. Its size is 5km by 4km. The colored dots indicate a mean degradation of the C/N_0 of at least -3dB. Underlaid is a shaded relief map derived from a digital surface model (DSM). Two main flight routes are visible in this area. The degradations on the right route reach values down to -18dB, while they do not decrease below -8dB on the left route. Attention has to be paid to the left route where the degradation systematically rises to values higher than -3dB at certain locations. One assumption for this behavior is that the helicopters might be shadowed from the RFI transmitter by obstacles, namely the terrain (including vegetation and buildings). This effect is the point of origin of this study. The concept is to trace back to the interference source by assessing the attenuation of the interfering signal caused among others by shadowing effects of the terrain and obstacles on ground.

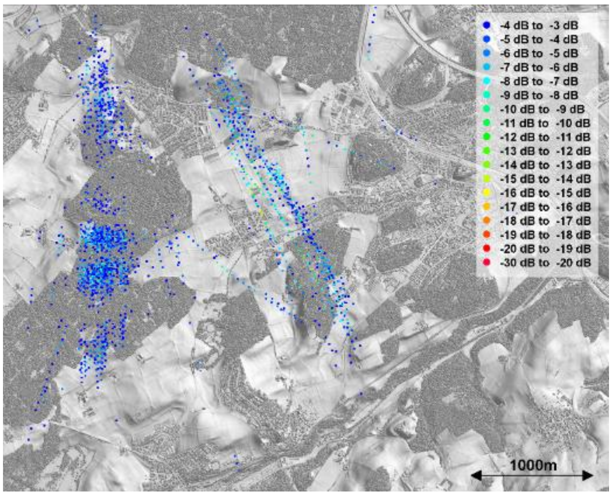

Figure 3: An area where the C/N_0 is repeatedly degraded indicating a potentially present RFI source.

CONCEPT FOR RFI TRANSMITTER LOCALIZATION

The concept for the localization of the RFI transmitter is to estimate the EIRP (Equivalent Isotropically Radiated Power) of this source based on the degradation of the C/N_0. It is obvious that different gains and losses of the interfering signal between RFI transmitter and GPS antenna have to be taken into account. Defining an arbitrary RFI transmitter position in the proximity of the affected flight paths allows to estimate the EIRP. In the most probable case the selected RFI transmitter position is incorrect and therefore the estimated EIRP varies from the effective EIRP. If a set of n affected helicopter positions is defined, which will further be denoted by the index i, then a set of $EIRP_i$ is estimated. The closer the arbitrary defined RFI transmitter position is to the real RFI transmitter position, the smaller is the variance of

$EIRP_i$. If additionally a set of m arbitrary RFI transmitter positions is defined, further denoted by an index j, then the problem can be reduced to find the j^{th} RFI transmitter position with minimum variance of $EIRP_i$, i.e.

$$min_j\{Var(EIRP_i)_j\}, i = 1..n, j = 1..m \quad (1)$$

RFI EIRP ESTIMATION

The effective carrier power to noise ratio $C_S/N_{0,eff}$ including an interfering signal can be approximated analytically by equation (2). An extensive treatment of following equation is given in [3].

$$C_S/N_{0,eff} = \left(\frac{1}{C/N_{0,exp}} + \frac{C_I/C_S}{QR_C}\right)^{-1} \quad (2)$$

where

- $C_S/N_{0,exp}$: expected carrier to noise power ratio of received GPS signal inside the receiver without any interfering signal,
- C_I/C_S: interfering to received GPS signal power ratio inside the GPS receiver
- Q: interference resistance quality factor
- R_C: chip rate of the Binary Phase Shift Keying (BPSK) code

The $C_S/N_{0,exp}$ is known through the empirically derived GPS receiver antenna pattern (see Figure 1). Analytical derivation of the dimensionless parameter Q is given in [3]. Q is approximately equal to 1 for CW (Continuous Wave) interfering signal at the L1 carrier frequency of 1.57542 GHz and increases when the CW frequency is shifted away, meaning that the GPS signal is then less affected. Q reaches values larger than 2 for a white noise like interfering signal. Finally, for the C/A code, R_C is equal to $1.023 \cdot 10^6$.

The EIRP of the RFI is derived based on equation (2) (see [3]) and expressed in dB-Hz yields

$$(C_S/N_0)_{eff,dB} = -10log_{10}\left[10^{-\frac{(C_S/N_0)_{exp,dB}}{10}} + \frac{10^{\frac{(C_I/C_S)_{dB}}{10}}}{QR_C}\right] \quad (3)$$

The round bracket followed by the index dB denotes, that the unit is dB. It follows

$$(C_I/C_S)_{dB} = 10log_{10}\left[QR_C\left(10^{-\frac{(C_S/N_0)_{eff,dB}}{10}} - 10^{-\frac{(C_S/N_0)_{exp,dB}}{10}}\right)\right] \quad (4)$$

Now, the measured degradation of the C/N_0 as shown in Figure 2 is brought into relation on the right side of equation (4). The left side of this equation can be expressed according to [3] as follows:

$$(C_I/C_S)_{dB} = (I_H/S_H)_{dB} + (G_{H,I})_{dB} - (G_{H,SVi})_{dB} \quad (5)$$

where

- I_H/S_H: interfering to GPS signal power ratio at the helicopter GPS antenna input
- $G_{H,SVi}$: helicopter GPS antenna gain towards ith GPS satellite
- $G_{H,I}$: helicopter GPS antenna gain towards interfering source

According to [4], the GPS signal power S_H at the helicopter GPS antenna for satellites of Block II to IIR is in the range of -158.5dBW to -156.5dBW. Both GPS antenna gains $G_{H,SVi}$ and $G_{H,I}$ can be omitted, as these parameters are already contained within the GPS antenna pattern for $C/N_{0,exp}$. The equations solved for I_H yield

$$(I_H)_{dB} = 10log_{10}\left[QR_C\left(10^{-\frac{(C_S/N_0)_{eff,dB}}{10}} - 10^{-\frac{(C_S/N_0)_{exp,dB}}{10}}\right)\right] - (S_H)_{dB} \quad (6)$$

The EIRP at the RFI source is therefore

$$(EIRP)_{dB} = (I_H)_{dB} - (G_I)_{dB} + (L_{FSPL})_{dB} + (L_{DIFF})_{dB} + (L_{POL})_{dB} + (L_{FE})_{dB} \quad (7)$$

Where

- G_I: RFI antenna gain towards helicopter
- L_{FSPL}: free space path loss of interfering signal
- L_{FIDD}: diffraction loss of interfering signal at the terrain and obstacles
- L_{POL}: loss due to polarization mismatch
- L_{FE}: loss due to receiver front end filtering

The RFI antenna gain G_I is unknown. A first approximation could be to assume a dipole antenna where the antenna gain can be derived. Another approach could be to assume a range of antenna gains and to derive a minimum and maximum EIRP based on the extremal values of this gain range. For instance, if an RFI dipole antenna is assumed, then a polarization mismatch between the linearly polarized RFI antenna and the right hand circularly polarized (RHCP) GPS antenna is present. This loss is taken into account within the parameter L_{POL}, which in this case would be 3dB. In case the interfering signal is out of band, a loss caused by the receiver front end filtering L_{FE} has to be taken into account. For the further discussion it is assumed that an in-band interfering signal is present yielding L_{FE} = 0dB.

The signal free space path loss L_{FSPL} is derived according to [5]

$$L_{FSPL} = 20log_{10}\left(\frac{4\pi d}{\lambda}\right) \quad (8)$$

where λ = 0.19m for the GPS L1 frequency. It is important that the distance d between RFI transmitter and GPS receiver antenna is derived from the arbitrarily selected RFI transmitter position as discussed in the chapter on the concept for RFI transmitter localization.

The loss caused by the signal diffraction L_{DIFF} is approximated by the Bullington method, which is an extension of the knife-edge loss method. This method is described and recommended in [6] where an automatic process is needed and in a situation where the terrain and obstacle profile is well known. The advantage of this method is the simple implementation in the simulation software used for this paper. However, it is also known that this method has the tendency to underestimate the diffraction loss.

The arbitrarily defined RFI transmitter locations are arranged in a grid with regular distances (e.g. 5m), and for each grid point the EIRP is calculated for each helicopter position with a degraded C/N_0. Therefore, for each grid point a set of n EIRP values is derived. The standard deviation of the EIRP values is used in order to find the correct RFI source position. The lower the standard deviation value, the closer the arbitrary position is to the correct RFI transmitter position. Nevertheless, outliers have to be expected, and hence more appropriate variables could be used as well, such as quantiles.

DIGITAL TERRAIN AND SURFACE MODELS

The calculation of the diffraction loss requires digital terrain models (DTM), or digital surface models (DSM), respectively. Today DTMs with a resolution of 1” or 3” in latitude and longitude are common, and in some cases freely available (e.g. Shuttle Radar Topography Model, SRTM). However, due to the relatively short distances between the RFI transmitter and the helicopter paths combined with obstacles (vegetation and buildings) with heights above ground of up to 30m or more, it is advantageous to rely on surface instead of terrain models. Further, higher horizontal resolutions lead to more accurate results.

Following DTM and DSM are at the disposition within this study

- DTM with 25m horizontal resolution (DHM25)
- DSM with 20m horizontal resolution (DOM20)
- DSM with 0.5m horizontal resolution (DOM-ZH)

where the DOM-ZH is used for the calculations and the other two are used for comparison of the results only. Figure 4 depicts the differences in resolution for these different digital models for an area of 500m by 500m containing buildings at the border of a small village (left), a farm house (middle/right), cultivated land (right) and forest (rear left). It is clearly visible that the high resolution surface model offers a great advantage for signal propagation calculation purposes.

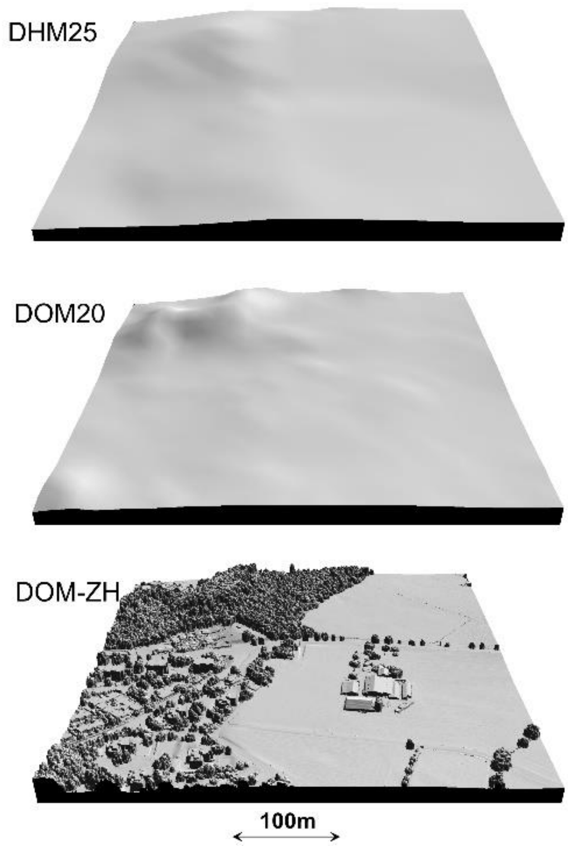

Figure 4: Comparison of one digital terrain model (top) and two digital surface models (middle and bottom) with different horizontal resolutions.

RESULTS

The situation depicted in Figure 3 is used as a test case. Some data is filtered in order to keep calculation time at a reasonable level. Only two flights are used, one for each route. Out of these two flights, only every tenth degraded C/N_0 is used, resulting in 17 samples (see black crosses in Figure 5). The grid space for the arbitrarily defined RFI transmitter locations is set to 5m. It is assumed that the RFI antenna is static and located 2m above the surface. The profile sampling for the signal diffraction estimation is set to 2m. For the RFI transmitter a half wavelength dipole antenna is assumed. Further, the RFI signal is assumed to be a CW within the GPS L1 band. The alternation of these RFI input parameters are discussed too.

The simulation result in Figure 5 shows that the potential location of the RFI transmitter can be dramatically confined to a few spots (red areas). These are the areas where EIRP's standard deviation is low, i.e. below a few mW. The areas with values larger than 10mW to 15mW are clipped.

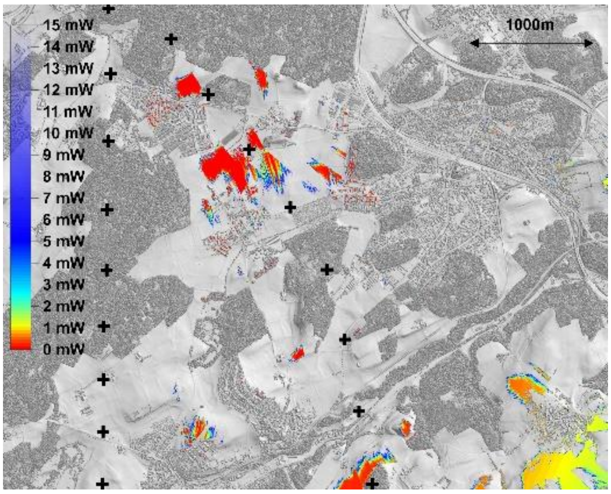

Figure 5: Potential areas where the RFI transmitter could be located.

Care has to be taken on the fact that very small areas of the size of buildings can be identified as potential RFI transmitter location as well (see Figure 6). This is due to the fact that the roofs of these buildings are more exposed to the flight paths than the nearby ground surface. Finally, artefacts can be detected within the forest. This is mainly due to the irregular shape of the DSM in this area. A screening with the help of a Geographic Information System (GIS) in order to find installed transmitting antennas in this area has shown, that only one of these antennas is located within the forest. Therefore, in a first step, the forest can be neglected as a search area for the RFI source.

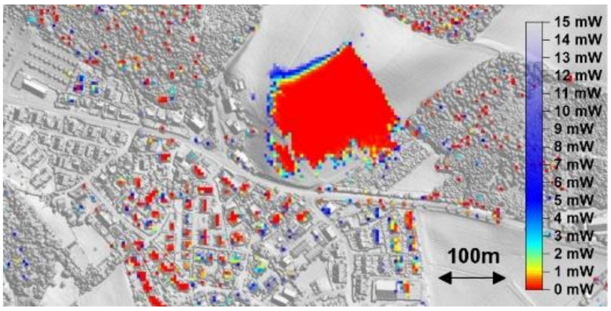

Figure 6: Detailed view of the left top part of Figure 5 showing the ability to identify single buildings as potential RFI transmitter location.

Variation of input parameters is performed in order to show that the result is only marginally affected by improper assumptions. This behavior can be explained by the fact that only the minimum standard deviation of the EIRP is assessed, but not the EIRP itself.

Two cases are discussed: Firstly, the assumed altitude of the RFI antenna over ground is increased from 2m to 5m. By consequence the RFI antenna will affect a larger area. Thus the area with the potentially correct position of the RFI transmitter increases, which is visible in Figure 7. However, when comparing this result with that in Figure 5, it can be seen that the area of interest is only slightly increased. This effect is advantageous in order to minimize the risk of searching the RFI transmitter in improper locations when assuming incorrect altitudes of the RFI antenna.

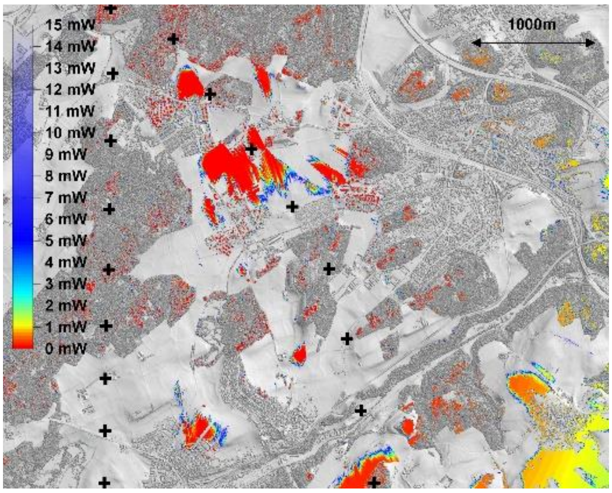

Figure 7: Potential areas where the RFI transmitter could be located. In this case the assumed altitude of the RFI antenna over ground is increased from 2m to 5m.

The second case assesses inappropriate assumption on the RFI signal characteristics, e.g. polarization of the interfering signal or out of band instead of in-band interference. To do this, an additional constant loss of 6dB is taken into account in equation (7). The assumed altitude of the RFI antenna over ground is set to 2m. This adaptation systematically affects the calculated EIRP. Nevertheless, the size of potential areas containing the RFI transmitter is only marginal affected, as can be seen in Figure 8. The range where the potential RFI transmitter could be located has to be increased. This is visible when comparing the right bottom part of the Figures 5 and 7.

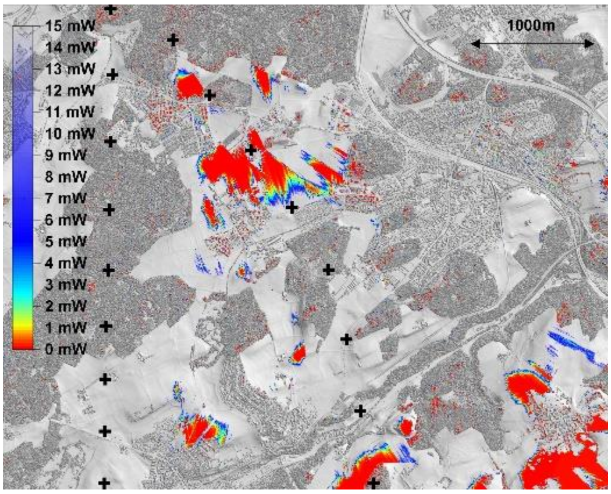

Figure 8: Potential areas where the RFI transmitter could be located. In this case the assumed altitude of the RFI antenna over ground is increased from 2m to 5m.

Finally, the impact on the results depending on selection of DSM and DTM is shown. Figure 9 depicts the result when applying a DTM with 25m horizontal resolution (DHM25) and within Figure 10 a DSM with 20m horizontal resolution (DOM20). The advantage of high resolution DSM is clearly visible when comparing these results with that in Figure 5. Even with similar horizontal resolutions (20m to 25m) a DSM has an advantage compared to a DTM.

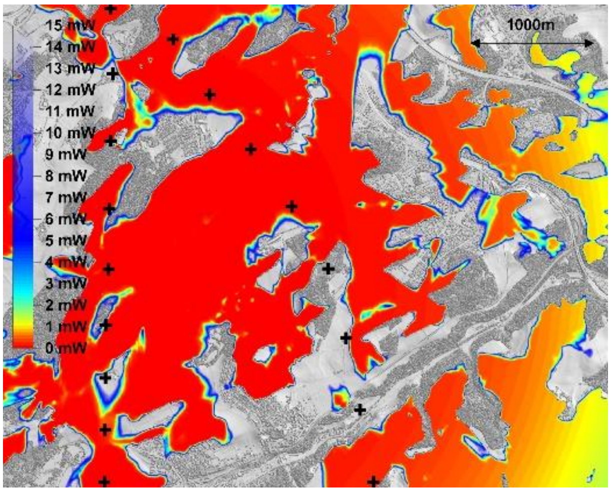

Figure 9: Simulation results when using a DTM with 25m horizontal resolution instead of a DSM with 0.5m horizontal resolution.

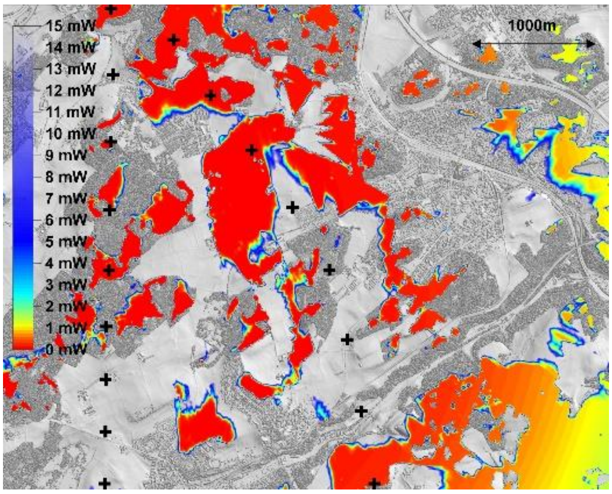

Figure 10: Simulation results when using a DSM with 20m horizontal resolution instead of a DSM with 0.5m horizontal resolution.

CONCLUSIONS

A method has been described which allows to confine the search area of a RFI transmitter site. This is based on the comparison between expected and effective C/N_0 while taking advantage of high resolution digital surface models. Following conclusions are deduced from this study:

a) The described method allows to reduce the search area of a RFI transmitter site to a large extent.

b) The use of high resolution digital surface models improve the result quality by several factors.

c) To a certain degree the results are not affected by inadequate assumptions on the RFI transmitter characteristics.

RECOMMENDATIONS

It is recommended to apply the presented method in order to reduce the search area of a static RFI transmitter and consequently to reduce the time to localize the RFI transmitter.

FUTURE WORK

Additional analysis will be performed on the signal diffraction loss models. Processing time and result quality shall be reasonably balanced.

The antenna pattern for the expected C/N_0 will be assessed more in detail for negative angles. Currently only limited data is available for each helicopter. Improvement of this parameter is particularly important when the helicopter flies close or over the RFI transmitter.

After having assessed the impact of the RFI transmitter in the spatial domain it is important to assess the temporal domain too. This additional information is crucial when attempting to localize the RFI transmitter on-site.

ACKNOWLEDGMENTS

Special thanks go to CHIPS and the Swiss Federal Office of Civil Aviation for the financial support of this project within the frame of the applied research and development programme for implementation of future navigation applications in Switzerland. Contributions to this study were done by P. Truffer, G. Aschwanden, H. Wipf, and M. Troller (skyguide), H. Leibundgut (REGA), S. Rämi, and M. Bertschi (Swiss Air Force), and R. Wittwer (armasuisse).

REFERENCES

[1] M. Scaramuzza, H. Wipf, M. Troller, H. Leibundgut, R. Wittwer, and S. Rämi, 2014, GNSS RFI Detection in Switzerland based on Helicopter Recording Random Flights, Proceedings of IFIS 2014, Oklahoma City, USA.

[2] M. Scaramuzza, H. Wipf, M. Troller, H. Leibundgut, S. Rämi and R. Wittwer, GNSS RFI Detection: Finding the Needle in the Haystack, Proceedings of ION GNSS Conference 2015 Tampa, Florida.

[3] P. Ward, J. Betz, and C. Hegarty, Interference, Multipath, and Scintillation, Chapter 6 in book 'Understanding GPS – Principles and Applications', 2nd Edition, Artec House, 2006.

[4] US DoD, Navstar GPS Space Segment/Navigation User Interfaces, Interface Specifications IS-GPS-200H, Global Positioning Systems Directorate, Systems Engineering & Integration, 24.9.2013.

[5] ITU, Calculation of Free-Space Attenuation, Recommendation, ITU-R P.525-2, 1994.

[6] ITU, Propagation by Diffraction, ITU-R P.526-13, 2013.